Eleven-Step Chemoenzymatic Synthesis of Cotylenol

Yanlong Jiang,[§] Hans Renata*,[§]

[§]Department of Chemistry, BioScience Research Collaborative, Rice University, Houston, TX, 77005, USA

ABSTRACT: Cotylenin A and fusicoccin A are two flagship members of the fusicoccane diterpenoid family that are capable of acting as molecular glues to stabilize the interaction between the 14-3-3 proteins and their clients. Herein, we report a concise chemoenzymatic synthesis of cotylenol, the aglycone of cotylenin A. Key features that contribute to the brevity of the route include the union of two cyclopentene fragments in an allylative coupling, a one-pot Prins cyclization-transannular hydride shift sequence, and a late-stage enzymatic oxidation to install the key tertiary alcohol at C3.

The fusicoccanes are fungal diterpenoids that are defined by their 5/8/5 ring system.[1] Several members of the family, such as cotylenin A (**1**) and derivatives of fusicoccin A (**2**), are known to induce apoptosis and act as "molecular glues" to stabilize the protein–protein interaction (PPI) between the 14-3-3 hub proteins and several of their partners.[2] The 14-3-3 proteins serve as adaptor proteins that regulate many cellular processes by binding to a variety of disease-relevant signaling proteins, such as Raf kinases and the YAP transcriptional modulator.[3] Given this role, there has been a widespread interest in the development of small molecules that are able to modulate these PPIs. Studies by Ottmann and others[4] on cotylenin A and related natural and semisynthetic fusicoccanes have begun to suggest that modulation of PPI between 14-3-3 proteins and different binding partners is possible by adjusting the oxidation patterns of the scaffold. Interestingly, studies by Ohkanda and co-workers have suggested that the absence of a secondary alcohol at C12 is a key molecular determinant for cellular cytotoxicity.[5] Though the sugar moieties contribute to a tighter ternary complex formation, they are not critical for activity.[6] X-ray diffraction studies lend further support to this observation as the sugar moieties are found to be partially solvent exposed in the crystal structures.[7] In agreement, cotylenol was observed to exhibit moderate cytotoxicity on human myeloid leukemia cells and a crystal structure of cotylenol in complex with 14-3-3σ and a synthetic C-terminal hexapeptide of TASK-3 has also been solved (PDB ID: 3SP5).[4]

Despite their promising biological activities, access to **1** and **3** has been challenging as their native fungal producer, *Cladosporium* sp. 501-7W, was reported to lose its ability to proliferate during preservation.[8] Recent efforts in the synthesis of the fusiccocanes notwithstanding,[9–11] *de novo* preparation of **1** and **3** has also proven nontrivial. To date, only two total syntheses of cotylenol have been reported so far, proceeding in 29 steps (Kato and Takeshita, 1996)[12] and 19 steps (Nakada, 2020) respectively.[13] Motivated by these synthetic shortcomings, we sought to develop a concise chemoenzymatic strategy to access cotylenol. In this Communication, we devised an eleven-step synthesis of **3**, which represents a significant improvement from previous syntheses. Additionally, this work provided the first foray towards establishing the biocatalytic utility and substrate promiscuity of the key dioxygenase from the native

biosynthetic pathway of cotylenol. Beyond cotylenol, this work also lays the foundation for a future family-level synthetic solution to brassicicene congeners, including those with alternative skeletal connectivities,[14] to enable further exploration into their pharmacological properties.
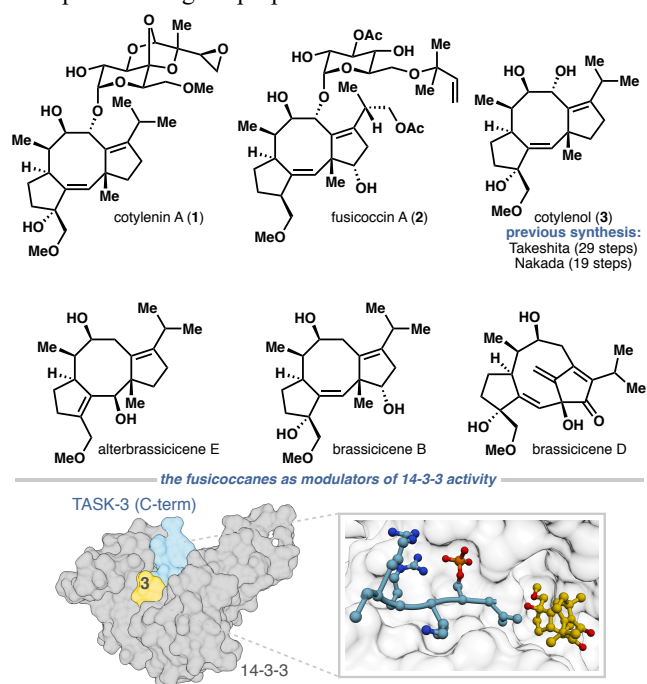

Figure 1. Representative members of the fusicoccane diterpenoid family and their activity as modulators of protein-protein interactions with the 14-3-3 adaptor proteins.

Our approach towards cotylenol hinges on several late-stage oxidative maneuvers to install the hydroxyl groups at C3, C8 and C9 in an expedient fashion. Based on Nakada's work, the C8,C9-*trans*-diol of **3** would be accessed from the C8-keto counterpart through judicious redox manipulations. In addition, we were aware of Dairi's and Oikawa's prior biosynthetic studies on **3** and the brassicicenes, which identified the role of the non-heme dioxygenases (NHDs) BscD and Bsc9 in the generation of the C3 alcohol.[8,15] In the native biosynthetic pathway, alcohol **8** undergoes an initial hydrogen atom abstraction at C1,

which leads to subsequent olefin isomerization and a net C–H oxidation at C3 to produce **9** along with the shunt product **10**. Though the synthetic application of BscD and Bsc9 has not been demonstrated, the biocatalytic oxidation transform was deemed strategic and worth the risk, especially in light of the challenges involved in installing the C3 alcohol in prior syntheses. In a further departure from the native biosynthetic pathway, our synthetic design would also apply the enzymatic oxidation on **5** instead of **8**. This decision posed an added risk as the substrate promiscuity of the enzymes have not been investigated. Nevertheless, the prospect of further minimizing unnecessary concession steps in the synthesis was viewed as a worthy tradeoff. Ketone **5** would arise from synthons **A** and **B** through two C–C bond forming events and the appropriate synthetic equivalents of **A** and **B** could be found in cyclopentenes **6** and **7**. In particular, Takeshita's prior use[12] of Nozaki-Hiyama-Kishi-based allylation serves as a strategic inspiration due to its ability to construct the key quaternary center at C11 with high stereoselectivity.
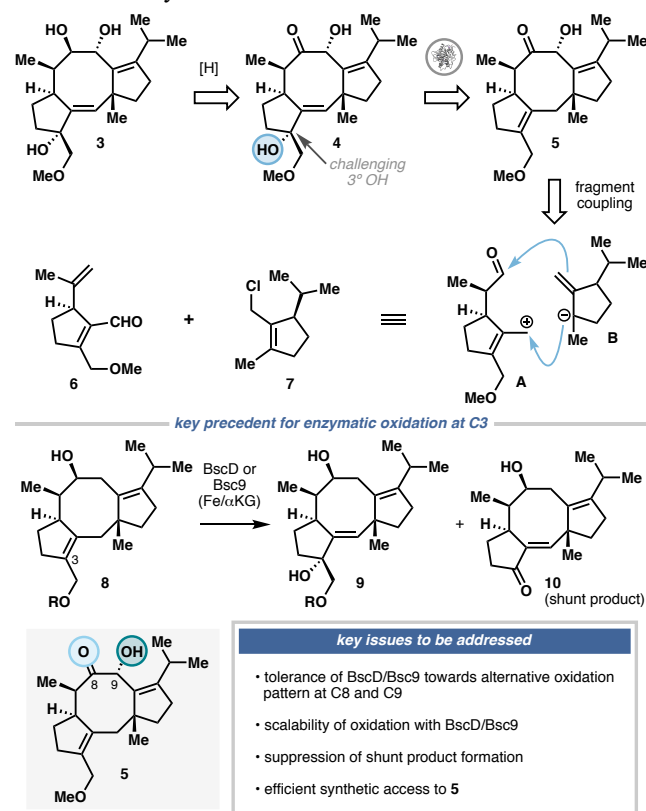

Figure 2. Retrosynthetic analysis of **3** featuring a late-stage enzymatic oxidation to install the challenging tertiary alcohol at C3 and the use of a fragment coupling to generate the general 5/8/5 tricyclic ring system.

The key cyclopentane fragments **6** and **7** were prepared in five steps each from (+)-limonene oxide (**11**) and (–)-limonene (**12**). Though simplified variants of **6** have previously been prepared from limonene, an efficient strategy to introduce the primary allylic alcohol has yet to be described. Towards this goal, **11** was subjected to a regioselective epoxide opening, followed by VO(acac)$_2$-catalyzed epoxidation to provide **13** as an inconsequential mixture of two stereoisomers. Treatment of this intermediate with NaOMe effected an epoxide ring opening from the less-hindered position and the resulting diol was oxidatively cleaved in the presence of NaIO$_4$. An intramolecular aldol condensation completed the synthesis of cyclopentenal **6**. This five-

step sequence could be routinely conducted on decagram scale with satisfactory overall yield (39%). Synthesis of intermediate **7** proceeded through a known compound, **16**, which was prepared through slight modifications of a known route.[16] Briefly, catalytic hydrogenation of the isopropenyl unit of **12** in the presence of PtO$_2$ and ozonolysis of its trisubstituted olefin furnished **15** in 72% yield. An intramolecular aldol condensation and aldehyde reduction generated alcohol **16**, which was chlorinated in the presence of (COCl)$_2$ and DMSO to complete the synthesis of **7**. Similar to the preparation of **6**, this five-step route proved to be robust, proceeding routinely on five-gram scale with 44% overall yield.

Union of **6** and **7** was realized by employing Fürstner's modification of the Nozaki-Hiyama-Kishi (NHK) reaction.[17] This method was chosen for two strategic reasons: (1) it features the catalytic use of low-valent chromium salt, which has been noted to pose physiological hazards, and (2) the use of TMSCl as the reaction mediator allowed for simultaneous capping of the C1 alcohol as the TMS ether. With regards to the latter feature, we observed in our initial forays that the free alcohol at C1 was not compatible with the subsequent hydroboration step and its protection also improved the yields of the latter steps. Selective hydroboration of the isopropenyl unit and oxidation of the corresponding primary alcohol to the aldehyde were combined in a telescoped protocol to afford **18**, whose stereochemical configuration was verified through single-crystal X-ray diffraction. Submission of this intermediate to a Prins reaction in the presence of BF$_3$•Et$_2$O generated a 5/8/5 tricycle that contains all the necessary chemical handles for accessing **3**. At this stage, the extraneous hydroxyl group at C1 needed to be excised. During our attempts to deprotect the TMS group, it was found that the use of TFA on **19** could lead to a complete deoxygenation at C1 along with the formation of a ketone moiety at C8. Though further studies are still needed, this transformation likely proceeds through selective ionization of the C1 hydroxyl group, which initiates a transannular hydride transfer from the C8 carbon.

Using the above discovery as a starting point, we looked to identify a suitable protocol to convert **18** to **20** in one step. An extensive test of Lewis and Brønsted acids for this conversion eventually led to the development of a one-pot protocol featuring an initial treatment with BF$_3$•Et$_2$O, followed by the addition of tetra-n-butylammonium bifluoride (TBABF), which likely reacts with BF$_3$ to generate HBF$_4$ in situ.[18] In comparison, stronger conditions tested led to simple elimination of the C1-OH (see Table S4 in the Supporting Information). Prior syntheses of **3** had established the viability of installing the C9 hydroxyl group via enolate α-oxidation with MoOPH. Due to safety and toxicity issues associated with preparing MoOPH[19] on large scale, an alternative set of conditions to effect this transformation was sought. After an extensive screening, it was found that a combination of LiOtBu and KH and molecular oxygen in the presence of P(OMe)$_3$ could be employed to afford **5** in high conversion, selectivity and isolated yield, though a minor byproduct arising from α-oxidation at C7 could also be observed (see Table S5 in the Supporting Information). As a testament to the scalability of the route, the entire sequence toward **5** could be routinely conducted on gram-scale or near gram-scale to provide ample material supply for our biocatalytic exploration of BscD and Bsc9.

While Bsc9 could be heterologously expressed as a N-His$_6$-tagged protein in *E. coli*, BscD was found to be completely insoluble. BscD and Bsc9 share ca. 70% sequence identity, and

the regions of divergence are primarily found in their N-terminal domains, in which Bsc9 contains an additional 26-residue sequence, and two insertion segments. Grafting of the N-terminal domain of Bsc9 onto BscD was attempted, but this effort did not lead to any improvement in soluble protein yield. Reaction of **5** with Bsc9 in cell lysates provided a mixture of the desired tertiary alcohol product (**4**) and shunt product **21** with moderate conversion. In accordance, no reaction was observed with *E. coli* lysates containing BscD. In their initial discovery of Bsc9,[8] Dairi and co-workers proposed that the shunt product arises from trapping of the tertiary radical at C3 with molecular

oxygen through the intermediacy of a dioxetane species. As no further mechanistic studies were performed by Dairi and co-workers, we sought to investigate whether **21** could have arisen from **4** via enzyme-assisted oxidative cleavage. From the perspective of reaction optimization, we speculated that if **21** is actually derived from **4**, the ratio of **4:21** could be readily modulated by adjusting the reaction conditions. Subjecting **4** to the enzymatic transformation provided no further conversion, disproving this hypothesis. Importantly, this observation suggested that optimization of the product composition in the reaction would have to be achieved through alternative means.

Scheme 1. A. Eleven-step chemoenzymatic synthesis of cotylenol (**3**). **B.** Optimization of enzymatic oxidation to convert **5** to **4** and **22** to brassicicene I (**23**) through homolog screening and directed evolution. Phylogenetic tree was generated by aligning the homologs on Clustal Omega and visualizing the alignment with iTOL.[20]
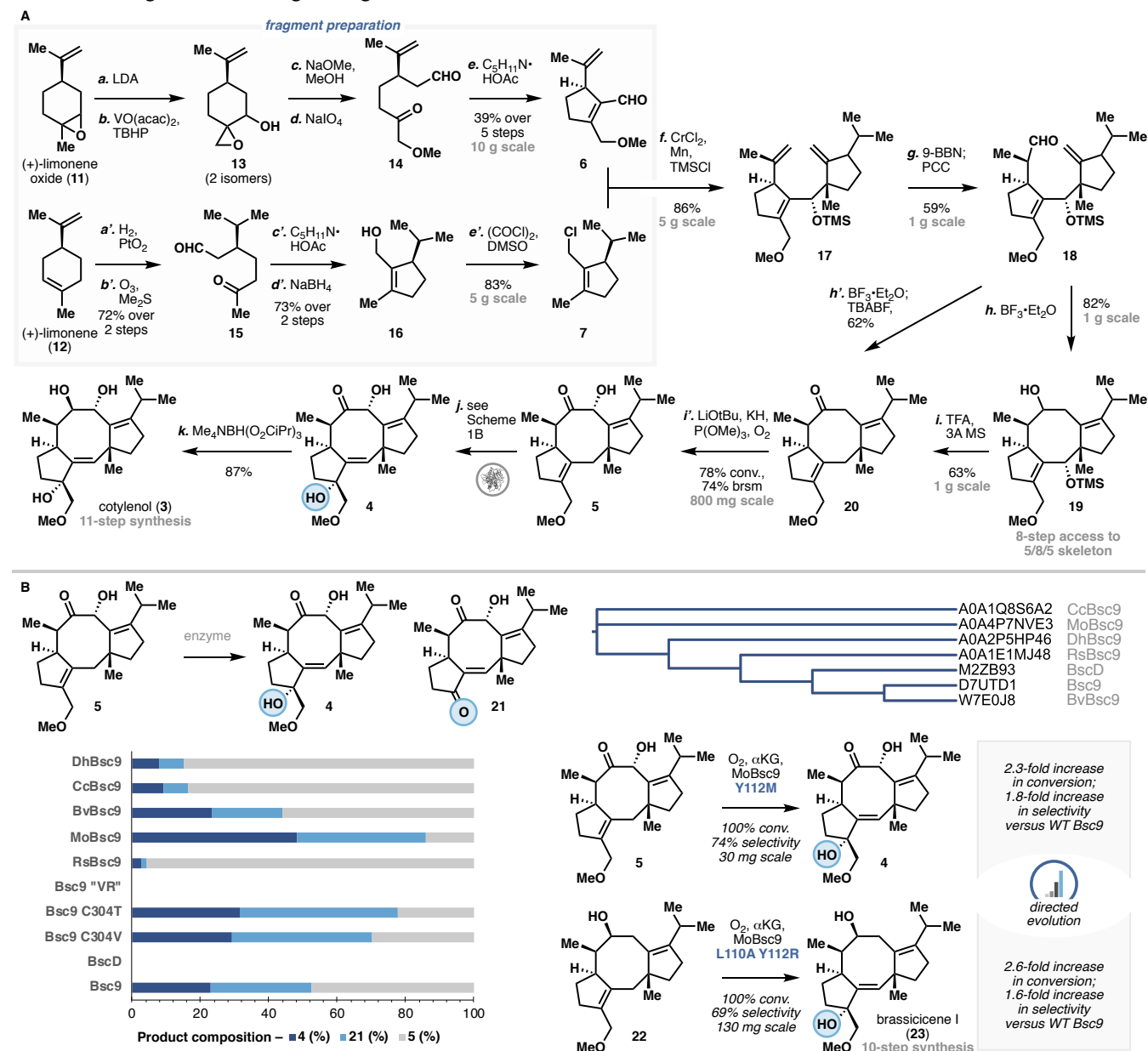
During our initial tests of Bsc9 in cell lysates, a large batch-to-batch variability of the reaction outcome was observed. Eventually, this issue was rectified by developing a consistent and rigorous lysis protocol and ensuring that the lysates were used immediately for reaction. Addition of TCEP to the lysate was also found to improve conversion. In line with this observation,

purified Bsc9 readily formed precipitates, suggesting rapid denaturation. Bsc9 contains two cysteine residues, one of which (C304) is predicted by homology model[21] to be surface exposed. We speculated that this residue could be targeted for mutagenesis to enhance the reaction outcome. While mutations C304V and C304T in Bsc9 resulted in small improvements in

conversion, the ratio of **4:21** did not improve. Our homology model also predicted that one of the insertion segments in Bsc9 (Ala103–Gly116, hereby referred to as "active-site insertion") lies opposite of the His-His-Asp iron-binding triad in the active site. As this region might be implicated in substrate binding, we generated a Bsc9-BscD chimera by swapping the Ala103–Gly116 sequence of Bsc9 with the corresponding Val-Arg diad from BscD. This chimera (Bsc "VR") provided no reaction on **5**, suggesting the importance of the active-site insertion segment for hydroxylation activity on **5**.

The above observation prompted us to test additional homologs of Bsc9 that diverge at the N-terminal and the active-site insertion region. Ten homologs were identified by picking the top ten hits from Genome Neighborhood Diagram (GND) analysis[22] and five of the ten were arbitrarily chosen for further characterization. Gratifyingly, a homolog from *Magnaporthe oryzae* (MoBsc9, 54% sequence identity to Bsc9) displayed improved conversion and ratio of **4:21**, which translates to *ca.* two-fold improvement in assay yield of **4**. Interestingly, no terpene synthase encoding genes could be identified within the vicinity of *MoBsc9*, suggesting that this dioxygenase might be involved in the biosynthesis of an entirely different natural product scaffold. Though the native function of this enzyme is still unclear to date, our discovery highlights the power of homolog screening in the unbiased discovery of superior enzyme(s) for a target reaction.

A brief directed evolution campaign was conducted to further improve the ratio of **4:21** in the enzymatic reaction. Based on our homology model of MoBsc9, two hydrophobic residues in the putative active site, L110 and Y112, were targeted for site-saturation mutagenesis. Reetz's "22-c trick" approach[23] to reduce codon redundancy was employed in combination with our previously-developed thin layer chromatography-based (TLC-based) screening strategy.[24] In this round of screening, we identified mutation Y112M that afforded 8% improvement in selectivity while maintaining the high reaction conversion. Concurrently, screening of the Y112X library for reaction with **22**, prepared via one-step reduction of **20**, yielded variant Y112R that produced brassicicene I (**23**) with 67% conversion and 51% selectivity (defined as percent ratio of the desired product : total products). As a comparison, WT Bsc9 provided only 37% conversion and 43% selectivity in this reaction. Using these two single mutants as parents, another round of evolution was performed by randomly mutagenizing L110. While only marginal improvement (less than 5%) could be obtained in testing the Y112M L110X library on **5**, the Y112R L110X library yielded variant L110A that further improved the selectivity for the production of **23** by 18%. Overall, our directed evolution campaign allowed for 2.3-fold improvement in conversion and 1.8-fold improvement in selectivity for the production of **4** and 2.6-fold improvement in conversion and 1.6-fold improvement in selectivity for the production of **23** relative to WT Bsc9. Preparative scale biocatalytic reaction on 30–50 mg scale with MoBsc9 Y112M could be conducted to afford **4** in 67% isolated yield. A corresponding reaction on **22** with MoBsc9 L110A Y112R on 100 mg scale provided brassicicene I (**23**) in 64% isolated yield. The final reduction to provide cotylenol proceeded uneventfully under Nakada's conditions,[13] completing the synthesis in 11 steps (longest linear sequence) from commercial materials. Additionally, we achieved the synthesis of brassicicene I in 10 steps from commercial materials.

To conclude, this work describes the development of a concise chemoenzymatic synthesis of cotylenol, which was achieved in just 11 steps. Salient features of our approach include the use of a catalytic NHK reaction for the union of two cyclopentane fragments that also set the key quaternary center at C11, the development of a one-pot Prins cyclization/transannular hydride transfer to construct the central cyclooctene ring of the target molecule, and the application of a late-stage enzymatic oxidation to generate the tertiary alcohol at C3. While Bsc9 provided unsatisfactory yield for this reaction, a superior enzyme that resulted in ca. 2-fold improvement in yield was identified through screening of additional homologs. This work provides a blueprint for developing a general and modular chemoenzymatic approach to other fusicoccanes bearing alternative oxidation patterns and functional groups to further structure-activity relationship studies on their ability to modulate 14-3-3 PPI.

ASSOCIATED CONTENT

Supporting Information

The Supporting Information is available free of charge on the Publications website.

Experimental details, analytical data, ^{1}H and ^{13}C NMR data (PDF).

AUTHOR INFORMATION

Corresponding Author

*hr28@rice.edu

Author Contributions

The manuscript was written through contributions of all authors. All authors have given approval to the final version of the manuscript.

ABBREVIATIONS

NHD, non-heme dioxygenase; VO(acac)$_2$, vanadyl acetylacetonate; DMSO, dimethylsulfoxide; TMS, trimethylsilyl; TBABF; *tert*-butylammonium bifluoride; MoOPh, oxodiperoxymolybdenum(pyridine)-(hexamethylphosphoric triamide).

REFERENCES

1. De Boer, A. H.; de Vries-van Leeuwen, I. J. Fusicoccanes; Diterpenes with surprising biological functions." *Trends Plant Sci.* **2012**, *17*, 360–368.
2. (a) Ohkanda, J. Fusicoccin: A chemical modulator for 14-3-3 proteins. *Chem. Lett.* **2021**, *50*, 57–67. (b) Marra, M.;

Camoni, L.; Visconti, S.; Fiorillo, A.; Evidente, A. The surprising story of fusicoccin: A wilt-inducing phytotoxin, a tool in plant physiology and a 14-3-3 targeted drug. *Biomolecules* **2021**, *11*, 1393. (c) Sengupta, A.; Liriano, J.; Bienkiewicz, E. A.; Miller, B. G.; Frederich, J. H. Probing the 14-3-3 isoform-specificity profile of protein-protein interactions stabilized by fusicoccin A. *ACS Omega* **2020**, *5*, 25029–25035.

3. Stevers, L. M.; Sijbesma, E.; Botta, M.; MacKintosh, C.; Obsil, T.; Landrieu, I.; Cau, Y.; Wilson, A. J.; Karawjczyk, A.; Eickhoff, J.; Davis, J.; Hann. M.; O'Mahony, G.; Doveston, R. G.; Brunsveld, L.; Ottman, C. Modulators of 14-3-3 protein-protein interactions. *J. Med. Chem.* **2018**, *61*, 3755–3778.

4. Anders, C.; Higuchi, Y.; Koschinsky, K.; Bartel, M.; Schumacher, B.; Thiel, P.; Nitta, H.; Preisig-Müller, R.; Schlichthöri, G.; Renigunta, V.; Ohkanda, J.; Daut, J.; Kato, N.; Ottmann, C. A semisynthetic fusicoccane stabilizes a protein-protein interaction and enhances the expression of K+ channels at the cell surface. *Chem. Biol.* **2013**, *20*, 583–593.

5. Ohkanda, J.; Kusumoto, A.; Punzalan, L.; Masuda, R.; Wang, C.; Parvatkar, P.; Akase, D.; Aida, M.; Uesugi, M.; Higuchi, Y.; Kato, N. Structural effect of fusicoccin upon upregulation of 14-3-3 phospholigand interaction and cytotoxic activity. *Chem. Eur. J.* **2018**, *24*, 16066–16071.

6. Asahi, K.; Honma, Y.; Hazeki, K.; Sassa, T.; Kubohara, Y.; Sakurai, A.; Takahashi, N. Cotylenin A, a plant-growth regulator, induces the differentiation in murine and human myeloid leukemia cells." *Biochem. Biophys. Res. Commun.* **1997**, *238*, 758–763.

7. (a) Ottmann, C.; Weyand, M.; Sassa, T.; Inoue, T.; Kato, N.; Wittinghofer, A.; Oecking, C. A structural rationale for selective stabilization of anti-tumor interactions of 14-3-3 proteins by cotylenin A. *J. Mol. Biol.* **2009**, *386*, 913–919. (b) Molzan, M.; Kasper, S.; Roglin, L.; Skwarczynska, M.; Sassa, T.; Inoue, T.; Breitenbuecher, F.; Ohkanda, J.; Kato, N.; Schuler, M.; Ottmann, C. Stabilization of physical RAF/14-3-3 interaction by cotylenin A as treatment strategy for RAS mutant cancers. *ACS Chem. Biol.* **2013**, *8*, 1869–1875.

8. Ono, Y.; Minami, A.; Noike, M.; Higuchi, Y.; Toyomasu, T.; Sassa, T.; Kato, N.; Dairi T. Dioxygenases, key enzymes to determine the aglycon structures of fusicoccin and brassicene, diterpene compounds produced by fungi. *J. Am. Chem. Soc.* **2011**, *133*, 2548–2555.

9. Williams, D. R.; Robinson, L. A.; Nevill, C. R.; Reddy, J. P. Strategies for the synthesis of fusicoccanes by Nazarov reactions of dolabelladienones: total synthesis of (+)-fusicoauritone. *Angew. Chem. Int. Ed.* **2007**, *46*, 915–918.

10. Chen, B.; Wu, Q.; Xu, D.; Zhang, X.; Ding, Y.; Bao, S.; Zhang, X.; Wang, L.; Chen, Y. A two-phase approach to fusicoccane synthesis to uncover a compound that reduces tumourigenesis in pancreatic cancer cells. *Angew. Chem. Int. Ed.* **2022**, DOI:10.1002/anie.202117476.

11. Wang, Y.-Q.; Xu, K.; Min, L.; Li, C.-C. Asymmetric total syntheses of hypoestin A, albolic acid, and ceroplastol II. *J. Am. Chem. Soc.* **2022**, DOI:10.1021/jacs.2c04633.

12. Kato, N.; Okamoto, H.; Takeshita, H. Total synthesis of optically active cotylenol, a fungal metabolite having a leaf growth activity. Intramolecular ene reaction for an eight-membered ring formation." *Tetrahedron* **1996**, *52*, 3921–3932.

13. Uwamori, M.; Osada, R.; Sugiyama, R.; Nagatani, K.; Nakada, M. Enantioselective total synthesis of cotylenin A." *J. Am. Chem. Soc.* **2020**, *142*, 5556–5561.

14. (a) Hu, Z.; Sun, W.; Li, F.; Guan. J.; Lu, Y.; Liu, J.; Tang, Y.; Du, G.; Xue, Y.; Luo, Z.; Wang, J.; Zhu, H.; Zhang, Y. Fusicoccane-derived diterpenoids from *Aternaria brassicicola*: Investigation of the structure-stability relationship and discovery of an IKKβ inhibitor. *Org. Lett.* **2018**, *20*, 5198–5202. (b) Li, F.; Lin, S.; Zhang, S.; Pan, L.; Chai, C.; Su, J.-C.; Yang. B.; Liu, J.; Wang, J.; Hu, Z.; Zhang, Y. Modified fusicoccane-type diterpenoids from *Alternaria brassicicola*. *J. Nat. Prod.* **2020**, *83*, 1931–1938. (c) Li, F.; Lin, S.; Zhang, S.; Hao, X.; Li, X.-N.; Yang. B.; Liu, J.; Wang, J.; Hu, Z.; Zhang, Y. Alterbrassinoids A–D: Fusicoccane-derived diterpenoid dimers featuring different carbon skeletons from *Alternaria brassicicola*. *Org. Lett.* **2019**, *21*, 8353–8357.

15. Tazawa, A.; Ye, Y.; Ozaki, T.; Liu, C.; Ogasawara, Y.; Dairi, T.; Higuchi, Y.; Kato, N.; Gomi, K.; Minami, A.; Oikawa, H. Total biosynthesis of brassicicenes: Identification of a key enzyme for skeletal diversification. *Org. Lett.* **2018**, *20*, 6178–6182.

16. (a) Lange, G. L.; Neider, E. E.; Orrom, W. J.; Wallace, D. J. Synthesis of the spirosesquiterpene (–)-acorenone and related cyclopentanoid monoterpenes. *Can. J. Chem.* **1978**, *56*, 1628–1633. (b) Mehta, G.; Krishnamurthy, N. An enantioselective approach to dolastane diterpenes. Total synthesis of marine natural products (+)-isoamijiol and (+)-dolasta-1(15),7,9-trien-14-ol. *Tetrahedron Lett.* **1987**, *28*, 5945–5948.

17. Fürstner, A.; Shi, N. Nozaki–Hiyama–Kishi reactions catalytic in chromium. *J. Am. Chem. Soc.* **1996**, *118*, 12349–12357.

18. Kilpatrick, M.; Luborsky, F. E. The conductance and vapor pressure of boron trifluoride in anhydrous hydrofuloric acid. *J. Am. Chem. Soc.* **1954**, *76*, 5865–5868.

19. Vedejs, E.; Engler, D. A.; Telschow, J. E. Transition-metal peroxide reactionsd. Synthesis of α-hydroxycarbonyl compounds from enolates. *J. Org. Chem.* **1978**, *43*, 188–196.

20. Letunic, I.; Bork, P. Interactive Tree Of Life (iTOL) v5: an online tool for phylogenetic tree display and annotation. *Nucleic Acids Res.* **2021**, *49*, W293–W296.

21. (a) Jumper, J. et al. Highly accurate protein structure prediction with AlphaFold. *Nature* **2021**, *596*, 583–589. (b) Baek, M.; DiMaio, F.; Anishchenko, I.; Dauparas, J.; Ovchinnikov, S.; Lee, G. R.; Wang, J.; Cong, Q.; Kinch, L. N.; Schaeffer, R. D.; Millán, C.; Park, H.; Adams, C.; Glassman, C. R.; DeGiovanni, A.; Pereira, J. H.; Rodrigues, A. V.; van Dijk, A. A.; Ebrecht, A. C.; Opperman, D. J.; Sagmeister, T.; Buhlheller, C.; Pavkov-Keller, T.; Rathinaswamy, M. K.; Dalwadi, U.; Yip, C. K.; Burke, J. E.; Garcia, K. C.; Grishin, N. V.; Adams, P. D.; Read, R. J.; Baker, D. Accurate prediction of protein structures and interactions using a three-track neural network. *Science*, **2021**, *373*, 871–876.

22. Zallot, R.; Oberg, N.; Gerlt, J. A. The EFI web resource for genomic enzymology tools: Leveraging protein, genome, and metagenome databases to discover novel enzymes and metabolic pathways. *Biochemistry* **2019**, *58*, 4169–4182.

23. Kille, S.; Acevedo-Rocha, C. G.; Parra, L. P.; Zhang, Z.-G.; Opperman, D. J.; Reetz, M. T.; Acevedo, J. P. Reducing codon redundancy and screening effort of combinatorial protein libraries created by saturation mutagenesis. *ACS Synth. Biol.* **2013**, *2*, 83–92.

24. Li, F.; Deng, H.; Renata, H. Remote B-ring oxidation of sclareol with an engineered P450 facilitates divergent access to complex terpenoids. *J. Am. Chem. Soc.* **2022**, *144*, 7616–7621.

Insert Table of Contents artwork here

Me

H,,

CHO

OMe

*5 steps from
(+)-limonene oxide*

Cl Me Me

Me

*5 steps from
(+)-limonene*

*late-stage
enzymatic oxidation*

*11-step longest
linear sequence*

Me OH Me

O Me

Me

H,,

Me

HO

MeO cotylenol